Society For Biomaterials

Scaffolding for challenging environments: Materials selection for tissue engineered intestine

Laura Boomer,[1] Yanchun Liu,[1] Nathan Mahler,[1] Jed Johnson,[2] Katelyn Zak,[2] Tyler Nelson,[3] John Lannutti,[3] Gail E. Besner[1]

[1]The Center for Perinatal Research, The Research Institute at Nationwide Children's Hospital, Department of Pediatric Surgery, The Ohio State University College of Medicine, Columbus, Ohio 43205
[2]Nanofiber Solutions, LLC, Columbus, Ohio 43212
[3]Department of Materials Science and Engineering, The Ohio State University, Columbus, Ohio

Received 11 October 2013; revised 12 November 2013; accepted 20 November 2013
Published online 00 Month 2013 in Wiley Online Library (wileyonlinelibrary.com). DOI: 10.1002/jbm.a.35047

Abstract: Novel therapies are crucially needed for short bowel syndrome. One potential therapy is the production of tissue engineered intestine (TEI). The intestinal environment presents significant challenges to the selection of appropriate material for tissue engineering scaffolds. Our goal was to characterize different scaffold materials to downselect to that best suited for TEI production. To investigate this, various tubular scaffolds were implanted into the peritoneal cavity of adult rats and harvested at multiple time-points. Harvested scaffolds were examined histologically and subjected to degradation studies and mechanical evaluation. We found that poly(glycolic acid) (PGA)-nanofiber and PGA-macrofiber scaffolds exhibited early robust tissue infiltration. Poly(ε-caprolactone) (PCL)-nanofiber, poly(L-lactic acid) (PLLA)-nanofiber, poly(D-lactic acid-*co*-glycolic acid) (PDLGA)-nanofiber and polyurethane (PU)-nanofiber experienced slower tissue infiltration. Poly(ε-caprolactone-*co*-lactic acid) (PLC) nanofiber had poor tissue infiltration. Significant weight loss was observed in PGA-nanofiber (92.2%), PGA-macrofiber (67.6%), and PDLGA-nanofiber (76.9%) scaffolds. Individual fibers were no longer seen by scanning electron microscopy in PLC-nanofiber and PGA-nanofiber scaffolds after 1 week, PGA-macrofiber scaffolds after 2 weeks, and PDLGA-nanofiber scaffolds after 4 weeks. In conclusion, PGA-macrofiber and PDLGA appear to be the most appropriate materials choices as TEI scaffolds due to their biocompatibility and degradation. Future experiments will confirm these results by analyzing cell-seeded scaffolds *in vitro* and *in vivo*. © 2013 Wiley Periodicals, Inc. J Biomed Mater Res Part A: 00A:000–000, 2013.

Key Words: tissue engineering, intestine, scaffolds, short bowel syndrome

How to cite this article: Boomer L, Liu Y, Mahler N, Johnson J, Zak K, Nelson T, Lannutti J, Besner GE. 2013. Scaffolding for challenging environments: Materials selection for tissue engineered intestine. J Biomed Mater Res Part A 2013: 00A: 000–000.

INTRODUCTION

Short bowel syndrome (SBS) is defined by metabolic and physiologic derangements, most often related to massive surgical resection. It is a significant medical problem associated with high morbidity and mortality, with a 5-year mortality in children approaching 30%.[1,2] Current treatment options include medical management with total parenteral nutrition (TPN), surgical procedures to try to enhance absorptive surface area or slow intestinal transit time, and autograft/allograft transplantation. Not only are these treatments suboptimal but both the cost and risk to the patient associated with current treatment options are high.[1] Novel therapies for this disease are clearly needed. The successful production of tissue engineered intestine (TEI) would avoid the problems associated with current therapies for SBS.

Tissue engineering, as opposed to transplant or mechanical replacement, has a goal of using the body's own regenerative capabilities to construct new, living tissues that do not require the use of antirejection or other medications.[3,4] To be successful, optimization of key components, namely cell source, biological environment, growth factors, and scaffold material, is required.[3,5,6]

The scaffold materials serve as a template, guiding implanted cells, and allowing them to proliferate and organize into desirable structures and tissues.[4] The features of scaffolds most crucial for production of TEI include designed levels of biodegradability, biocompatibility, strength, and elasticity comparable to that of the small intestine.[3] While scaffolds currently in use are fabricated from both natural and synthetic materials, the wide variability in the mechanical properties of synthetic materials made them attractive initial targets as scaffolds for TEI production.[7] Therefore, we chose to focus our initial studies on optimization of synthetic scaffold material. To date, a detailed evaluation of the numerous potential scaffold materials that can be used for the production of TEI has not been conducted. The purpose of this study was to characterize seven different scaffold materials to determine which would be best suited for TEI production.

Correspondence to: G. E. Besner; e-mail: gail.besner@nationwidechildrens.org

TABLE I. Characteristics of Polymers

Polymer	Molecular Formula	Density (g/cm3)	Melting Point	Tensile Modulus of Elasticity (GPa)	Tensile Strength (MPa)	Elongation at Break (%)	Degradation Time (mo)
PGA	$(C_2H_2O_2)_n$	1.5	225°C–230°C	6.5–7.0	90–110	1–2	6–12
PCL	$(C_6H_{10}O_2)_n$	1.2	60°C	0.2–0.3	25–35	>300	>24
PLC	$((C_3H_4O_2)$–$(C_6H_{10}O_2))_n$	1.25	110°C–120°C	0.02-0.04	18–22	>100	12–24
PLLA	$(C_3H_4O_2)_n$	1.3	150°C–160°C	3.1–3.7	60–70	2–6	>24
PDLGA	$((C_3H_4O_2)$–$(C_2H_2O_2))_n$	1.4	Amorphous	3.4–3.8	40–50	1–4	1–2
PU	$((C_{16}H_{14}O_3)_x$–$(C_{15}H_{14}O_2))_n$	1.2	180°C	0.03	45–50	>500	Biostable

MATERIALS AND METHODS

Animal care

All animal use and procedures were carried out in accordance with the Guide for the Care and Use of Laboratory Animals as proscribed by the National Institutes of Health. The protocol was approved by the Institutional Animal Care and Use Committee (IACUC) at the Research Institute at Nationwide Children's Hospital (protocol #AR12-00001).

Scaffold preparation

Two-millimeter thickness nonwoven poly(glycolic acid) (PGA) (Biomedical Structures, Warwick, RI) was obtained in sheet form, and was fashioned into tubes (5 cm in length, 5 mm in diameter) to create the PGA-macrofiber scaffolds. The PGA was cut to 1 cm × 2 cm and wrapped around a stainless steel mandrel along the length and sealed with 5% poly-L-lactic acid (Sigma-Aldrich, St. Louis, MO) in chloroform (Sigma-Aldrich, St. Louis, MO).[8] The scaffolds were kept in a laminar flow hood for 12 hr to allow the chloroform to completely evaporate.

Six additional nanofiber scaffold materials were manufactured by Nanofiber Solutions, LLC (Columbus, OH) via electrospinning. Polymers used for construction of the nanofiber scaffolds included PGA, poly(ε-caprolactone) (PCL), poly(ε-caprolactone-*co*-lactic acid) (PLC), poly(L-lactic acid) (PLLA), poly(D-lactic acid-co-glycolic acid) (PDLGA), and polyurethane (PU). The physical and chemical characteristics of these polymers are shown in Table I. Polymer solutions were prepared by dissolution in organic solvents mixed by a magnetic stir bar for 12 hr. Briefly, a 5 wt % solution of PCL or PLC in 1,1,1,3,3,3-hexafluoro-2-propanol (HFIP) was prepared by continuous stirring at room temperature. This solution was placed in a 60 mL syringe with a 20 gauge blunt tip needle and electrospun using a high voltage DC power supply (Glassman High Voltage, Inc., High Bridge, NJ) set to +16 kV, a 20 cm tip-to-substrate distance[9] and a 5 mL/hr flow rate. Nanofiber was deposited onto a rotating 4.76 mm diameter stainless steel rod until the desired wall thickness was reached. A total sidewall thickness of 0.5 mm was achieved. The scaffold tubes were then removed from the rod and placed under vacuum to ensure removal of residual organic solvent.[10] Finally, the scaffold tubes were plasma treated to promote cellular attachment.[11]

These tubular scaffolds were then weighed and cut to desired lengths. One centimeter long tubes were used for degradation, histology, and scanning electron microscopy (SEM) studies. Tubes 4 cm in length were used for tensile strength studies. Tubes 2 cm in length were used for suture retention testing. Scaffolds for *in vivo* implantation were sterilized and maintained at −20°C until implantation. PGA-nanofiber, PGA-macrofiber, PLLA-nanofiber, PDLGA-nanofiber, and PU-nanofiber scaffolds were sterilized via exposure to hydrogen peroxide gas (Sterrad). PCL-nanofiber and PLC-nanofiber scaffolds were sterilized by immersion in 70% ethanol solution for 30 min, followed by three washes with sterile deionized water and freeze drying.

In vitro studies

Three 0.5 cm length tubular scaffolds were prepared from each of the seven scaffold materials and baseline weights obtained for *in vitro* testing. Scaffolds were placed in a 5 mL tube filled with 2 mL of simulated intestinal fluid (SIF, 50 m*M* KH_2PO_4, 22.4 m*M* NaOH, pH = 6.8) at 37°C under rotational agitation. At weekly intervals, all scaffolds were removed from the SIF, washed three times in distilled water, and freeze-dried overnight. Weights were recorded and the scaffolds re-exposed to SIF. This process was continued for a total of 12 weeks. The percentage of weight loss, used to estimate scaffold degradation, was calculated.

In vivo studies: degradation and histology

Surgical procedures. Lewis rats (Harlan Laboratories, Indianapolis, IN) weighing 200–400 g were used to study the effects of *in vivo* implantation. Under general anesthesia with inhalation of isofluorane, a midline laparotomy was performed and a 1 cm length of each of the seven scaffolds was secured to the anterior abdominal wall of the peritoneal cavity using 5-0 polypropylene suture. Three scaffolds were placed on either side of the midline and one in the pelvis [Fig. 1(A)]. Each scaffold was secured with two 5-0 polypropylene sutures passed through the lumen of the scaffold and then secured to the fascia. Animals were euthanized by CO_2 asphyxiation and scaffolds harvested at each of six time points (1, 2, 3, 4, 8, and 12 weeks) [Fig. 1(B)] were used for histological evaluation ($n = 3$), weight changes and SEM examination ($n = 3$).

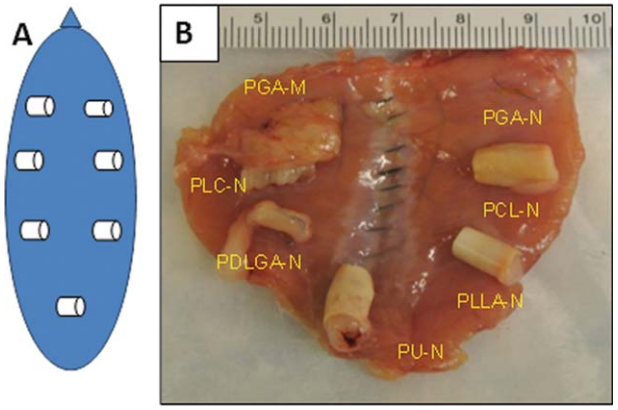

FIGURE 1. Scaffold implantation *in vivo*. (A) Schematic of scaffold orientation *in vivo*. (B) The abdominal wall after harvesting at 4 weeks showing scaffolds secured in their location against the underside of the abdominal wall. Poly(glycolic acid)-macrofiber (PGA-M), PGA-nanofiber (PGA-N), poly(ε-caprolactone-*co*-lactic acid)-nanofiber (PLC-N), poly(ε-caprolactone)-nanofiber (PCL-N), poly(D-lactic acid-*co*-glycolic acid) (PDLGA-N), poly(L-lactic acid)-nanofiber (PLLA-N), and polyurethane-nanofiber (PU-N). [Color figure can be viewed in the online issue, which is available at wileyonlinelibrary.com.]

Histology. Scaffolds were harvested *en bloc*, cut in a cross-sectional fashion across the center of the scaffold, fixed in 10% neutral buffered formalin, embedded in paraffin. Three sections were obtained from each of three levels at 200 μm intervals, deparaffinized in Americlear (Cardinal Health, Dublin, OH), and stained with hematoxylin and eosin (H&E) dye. Slides were examined and assessed microscopically.

Weight loss following* in vivo *exposure. Scaffolds to be used for degradation analysis were harvested and the ingrown tissue manually dissected free from the polymeric material. Scaffolds were cut into four to six pieces and placed into 4 mL of 5% sodium hypochlorite (Sigma-Aldrich, St. Louis, MO) diluted with phosphate buffered saline (PBS), to remove in-growth tissues. After digestion of adherent biological tissue in sodium hypochlorite, the scaffolds were rinsed five times in distilled water and freeze dried overnight. Each sample was then weighed to determine the amount of scaffold degradation as assessed by the change in weight preimplantation. Each of the seven scaffold materials were examined in triplicate at each time point and the percentage of weight loss was calculated.

Scanning electron microscopy (SEM). A portion of each of the samples used for scaffold degradation studies was gold sputter-coated (Emitech K550X, Quorum Technologies Ltd, Ashford, Kent, England) and examined by SEM (Hitachi S-4800, Hitachi High Technologies America, Inc., Dallas, TX) at a voltage of 7 kV at 100, 500, and 1000× magnification. Measurements of fiber diameter were taken from the SEM micrographs at random locations at 500× magnification using Image J software (National Institutes of Health, Bethesda, MD) from three different scaffold samples representing each time point.

***In vivo* studies: tensile strength and suture retention**

Surgical procedures. Additional adult male Lewis rats were anesthetized with isofluorane and a midline laparotomy made in order to implant longer scaffolds for tensile strength and suture retention testing. For tensile strength testing, two 4 cm scaffolds were placed into the peritoneal cavity, one on each side of the midline, and secured to the fascia with 5-0 polypropylene sutures ($n = 3$ scaffolds for each polymer). For suture retention testing, four 2 cm scaffolds were placed in the peritoneal cavity, two on each side of the midline, and secured ($n = 3$ scaffolds for each polymer). Three weeks later, the animals were euthanized by CO_2 asphyxiation and the scaffolds harvested.

Tensile strength determination. A Test Resources load frame (Model # SM-50-294-Capacity 50 lb, Northbrook, IL) was used for all measurements. The 4 cm long scaffolds from each of the six materials (PGA-macrofiber, PCL-nanofiber, PLC-nanofiber, PDLGA-nanofiber, PLLA-nanofiber, and PU nanofiber) were sterilized and subjected to tensile testing to obtain initial baseline strength values. Three 4 cm long scaffolds of each tested material were placed into PBS immediately after harvesting and stored on ice until testing. The PGA-nanofiber sample was not included due to its complete dissolution at 3 weeks *in vivo*. The width and thickness of each scaffold was measured using a digital micrometer. In each case, sufficient load was applied to the scaffold to eventually cause failure.

Suture retention testing. The 2 cm long scaffolds from the same six materials used for tensile strength testing were sterilized and used to determine baseline suture retention strength (SRS). The SRS of 2 cm long scaffolds ($n = 3$) from each material harvested after 3 weeks was compared with this baseline. These materials were placed in PBS immediately after harvesting and kept on ice until testing. The width and thickness of the scaffolds were measured using a digital micrometer. Three sutures (4-0 silk with a cutting needle) (Ethicon, Somerville, NJ) were placed 2 mm from the end of the scaffold, as previously described.[12] Each suture was tied with six knots. The tails of the sutures were cut at 5-cm length, and the group of them secured together with tape, to apply an even load to the samples. The secured sutures and the other end of the scaffold were placed into the grips of the load frame using a 50 lb load cell (Test Resources, Northbrook, IL). Load was applied at 50 mm/min until failure as determined by the suture pulling through the wall of the scaffold, and the stress–strain curve recorded.

Statistical analyses. Statistical analyses were performed using a two-way analysis of variance (ANOVA) for degradation analysis, one-way ANOVA for suture retention and tensile strength analysis, and Student's *t*-test for changes in individual scaffold materials from baseline, using SigmaPlot 12 software (Systat Software Inc, San Jose, CA).

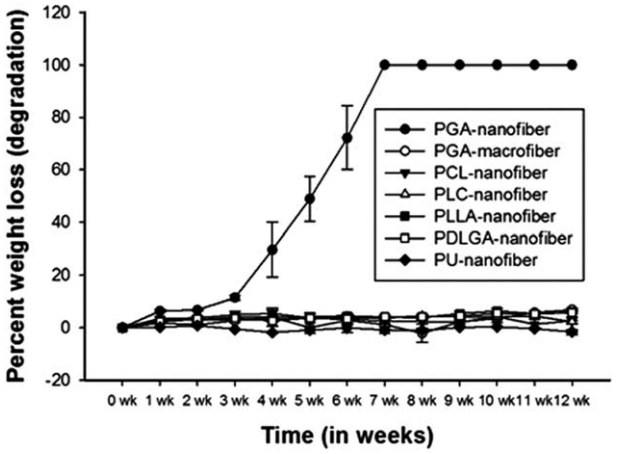

FIGURE 2. *In vitro* degradation rate. The percent of weight loss for each scaffold over 12 weeks of incubation in simulated intestinal fluid. Only the PGA-nanofiber displays significant weight loss over this period.

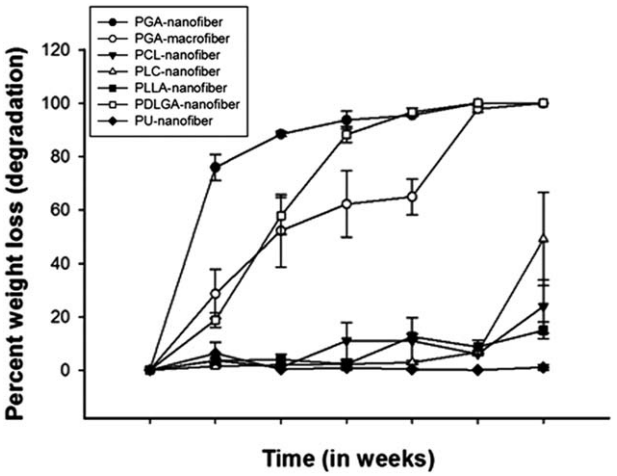

FIGURE 3. *In vivo* degradation rate. Weight loss over a 12 week incubation period after intraperitoneal implantation. Both the PGA- and PDLGA-nanofiber as well as the PGA-macrofiber display significant weight loss over the period.

RESULTS

In vitro degradation in simulated intestinal fluid

For the *in vitro* portion of the study, the degradation rate of each scaffold type was assessed by weekly measurements of change in scaffold weight over the 12-week incubation period. The PGA-nanofiber was the only composition that underwent significant, measurable change and showed complete degradation by week 8. All other materials displayed little weight change (Fig. 2). Several of the weekly measurements suggested a slight weight gain. This was attributed to solute from the SIF solution that remained trapped in the nanoscaled scaffold pores even after multiple rinses.

In vivo degradation after peritoneal implantation

At the end of the 12 week period of *in vivo* implantation, significant weight loss was identified for PGA-nanofiber (92.2% $\pm$ 9.3%), PDLGA-nanofiber (76.9% $\pm$ 31.0%), and PGA-macrofiber (67.6% $\pm$ 28.8%) scaffolds as opposed to PLC-nanofiber (10.7% $\pm$ 20.6%), PCL-nanofiber (9.4% $\pm$ 11.8%), PLLA-nanofiber (7.6% $\pm$ 5.7%), and PU-nanofiber (1.5% $\pm$ 3.4%) (all $p < 0.05$) (Fig. 3) when combining the percent weight loss for scaffolds at all of the time points. In addition to having significantly higher weight loss, PGA-nanofiber, PDLGA-nanofiber, and PGA-macrofiber had the bulk of the weight loss during the earlier time points, when compared with the other scaffold materials.

Histology

Histologic examination of the H&E stained scaffolds from the *in vivo* implantation is shown in Figure 4. PGA-nanofiber scaffolds showed significant tissue infiltration and fiber degradation as early as 1 week postimplantation; all of the nanofibers appeared to be absorbed following 4 weeks of implantation. There was marked tissue reaction with granulomatous inflammation at 2 weeks postimplantation, with numerous macrophages and a few foreign body giant cells. A reduction in the inflammatory reaction was observed, as the fibers were absorbed at 4 weeks postimplantation.

PGA-macrofiber scaffolds also showed significant, early tissue infiltration, but maintained structural integrity for longer periods of time. Fiber degradation was observed beginning at 21 days postimplantation. There was marked foreign body reaction at 2 weeks postimplantation again characterized by numerous foreign body giant cells and macrophages. Fibrosis located within the midpoint of the scaffold wall was observed at 2 weeks.

PCL-nanofiber scaffolds displayed slower tissue infiltration that became more prominent at 2–3 weeks accompanied better maintenance of structural integrity. There was foreign body reaction by 2 weeks postimplantation and fibrosis was observed starting at 3 weeks, and remained visible up to 12 weeks postimplantation.

PLC-nanofiber scaffolds showed poor tissue infiltration. The tissue reaction was characterized generally by chronic inflammation and fibrosis. Mild chronic inflammation was also present at 4, 8, and 12 weeks.

PLLA-nanofiber scaffolds also showed slower tissue infiltration that was not visible until at least 3 weeks postimplantation. The tissue reaction was characterized by mild chronic inflammation present throughout all time points; marked fibrosis was observed beginning at 3 weeks postimplantation. Fibers remained visibly intact up to 12 weeks postimplantation.

PDLGA-nanofiber scaffolds underwent slightly slower tissue infiltration at 2 weeks but rapid structural loss at 3–4 weeks. The tissue reaction was characterized by inflammation and fibrosis, both of which were mild at 1–2 weeks postimplantation and more chronic at 3–4 weeks. This was followed by a reduction in the inflammatory reaction as fibers were absorbed beginning at 4 weeks postimplantation. Degradation of fibers was visible at 1 week; fibers were essentially completely absorbed by 4 weeks postimplantation.

PU-nanofiber scaffolds exhibited tissue infiltration at 3–4 weeks but maintained structural integrity at all time points. The tissue reaction was characterized generally by

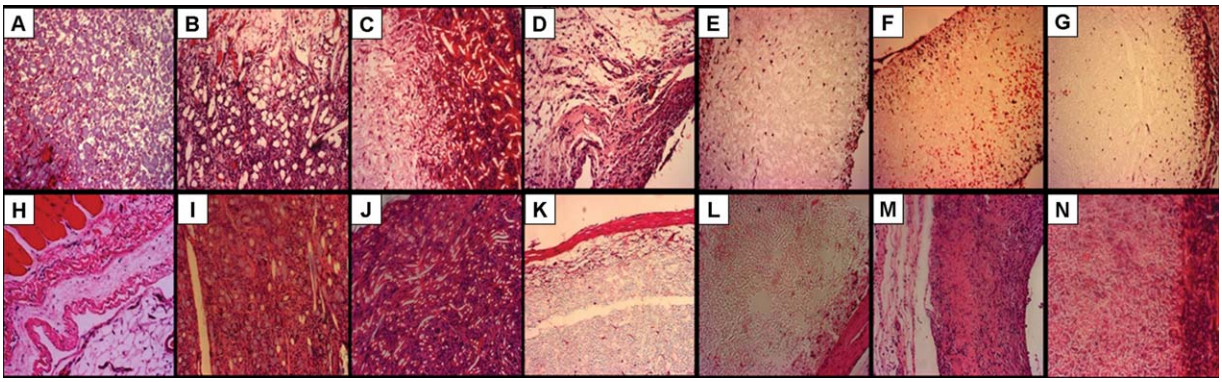

FIGURE 4. Histologic examination of scaffolds. Representative photomicrographs of H&E stained sections of each of the seven scaffolds (A–G) 1 week and (H–N) 4 weeks after implantation. (A,H) PGA-nanofiber: significant tissue infiltration begins at 1 week and no fibers are visible at 4 weeks; (B,I) PGA-macrofiber: significant tissue infiltration is visible starting at 1 week; some fibers remain visible at 4 weeks; (C,J) PCL-nanofiber: significant tissue infiltration and retained fiber structure are visible at 4 weeks; (D,K) PLC-nanofiber: minimal tissue infiltration and minimal degradation; (E,L) PLLA-nanofiber: almost no tissue infiltration and minimal degradation; (F,M) PDLGA-nanofiber: less tissue infiltration at 1 week but rapid degradation by 4 weeks; (G,N) PU-nanofiber: some tissue infiltration and no fiber degradation at 4 weeks.

chronic inflammation and fibrosis. The chronic tissue reaction transitioned to a foreign body reaction and fibrosis at 4 weeks postimplantation. Visibly undamaged fibers were present up to 12 weeks postimplantation.

Scanning electron microscopy (SEM)

SEM was performed for each of the scaffolds at each time point (Fig. 5). Individual fibers could not be distinguished for all PLC-nanofiber scaffolds, for PGA-nanofiber scaffolds at 1 week postimplantation, for PGA-macrofiber scaffolds at 2 weeks, and for PDLGA-nanofiber scaffolds at 4 weeks. Little change in fiber size, structure, or pore size was seen in PCL-nanofiber, PLLA-nanofiber, and PU-nanofiber scaffolds. PDLGA-nanofiber scaffolds underwent significant microstructural changes including increased pore size and individual fiber breakage at 2 weeks.

Tensile strength

Tensile strength measurements were taken for native small intestine, as well as for each of the six scaffold materials (PGA-macrofiber, PCL-nanofiber, PLC-nanofiber, PLLA-nanofiber, PDLGA-nanofiber, and PU-nanofiber) at baseline and after 3 weeks of intra-abdominal implantation (Fig. 6). PGA-nanofiber scaffolds were not used for testing of tensile strength due to near complete degradation at the 3 week time point. There was a statistically significant reduction in ultimate tensile strength (UTS) after implantation compared with baseline for PGA-macrofiber ($p < 0.001$), PCL-nanofiber ($p = 0.001$), PDLGA-nanofiber ($p < 0.001$), and PU-nanofiber ($p = 0.01$). There was also a statistically significant reduction in percent elongation after implantation compared with baseline for PGA-macrofiber ($p = 0.002$), PCL-nanofiber ($p = 0.003$), PDLGA-nanofiber ($p = 0.018$), and PU-nanofiber ($p < 0.001$). There was a statistically significant reduction in Young's modulus after implantation compared with baseline for PGA-macrofiber ($p < 0.001$), PCL-nanofiber ($p < 0.001$), and PDLGA-nanofiber ($p = 0.003$).

In addition, the mechanical properties of native small intestine were compared with each of the scaffolds at 3 weeks; no statistically significant differences in UTS were apparent. There was a statistically significant difference between percent elongation and PU-nanofiber compared with native small bowel, as well as each of the other five scaffolds ($p < 0.03$), but no significant differences between the other scaffolds and the native small bowel. PLLA-nanofiber and PLC-nanofiber had significantly higher Young's modulus when compared with native small bowel ($p = 0.003$), but no other significant differences could be identified.

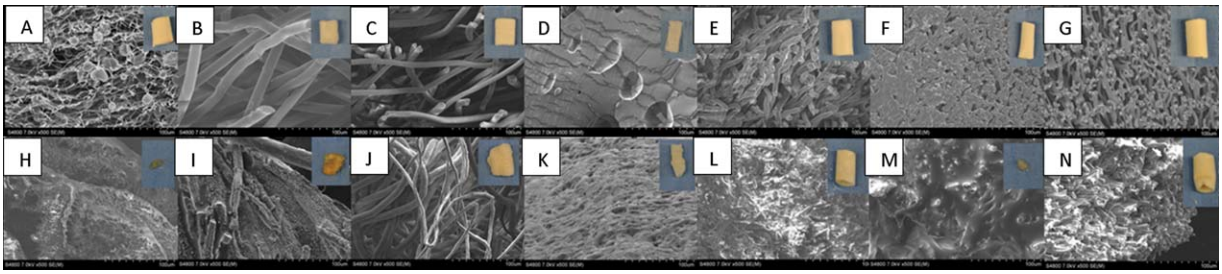

FIGURE 5. Scanning electron microscopic examination of scaffolds. SEM images (500×) of scaffolds (A–G) prior to implantation and (H–N) 4 weeks days after implantation. (A,H) PGA-nanofiber; (B,I) PGA-macrofiber; (C,J) PCL-nanofiber; (D,K) PLC-nanofiber; (E,L) PLLA-nanofiber; (F,M) PDLGA-nanofiber; and (G,N) PU-nanofiber. Insets show gross scaffold appearance. [Color figure can be viewed in the online issue, which is available at wileyonlinelibrary.com.]

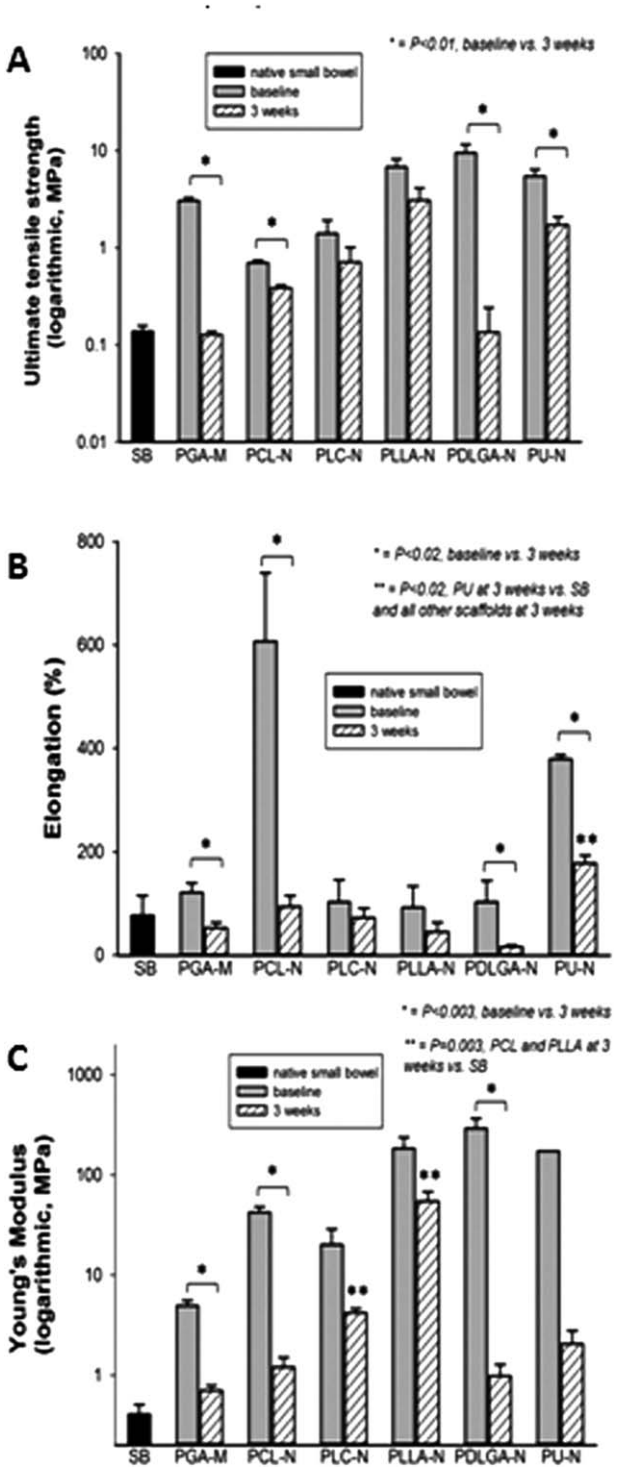

FIGURE 6. Tensile strength measurements. Tensile strength measurements are shown for native small bowel, and for scaffolds both prior to and after 3 weeks of implantation. (A) Ultimate tensile strength; (B) percent elongation; (C) Young's modulus. SB, small bowel; M, macrofiber; N, nanofiber.

Suture retention

SRS was evaluated for native small intestine and each of six scaffolds at baseline and after 3 weeks of intra-abdominal implantation (Fig. 7). PGA-nanofiber scaffolds were not used for SRS testing due to nearly complete degradation at the 3-week time point. Maximum force was calculated in Newtons for the small intestine samples as well as for each of the samples. There was a statistically significant reduction in SRS after 3 weeks of implantation for PGA-macrofiber ($p < 0.001$), PDLGA-nanofiber ($p < 0.001$), and PU-nanofiber ($p = 0.02$).

The maximum force for each scaffold after 3 weeks of implantation was also compared with that of the small intestine samples. PLC-nanofiber, PLLA-nanofiber, and PU-nanofiber all had significantly higher SRS than native small bowel following 3 weeks of intra-abdominal implantation ($p < 0.05$ for each). There was no statistically significant difference between native small intestine and the other three scaffolds after 3 weeks of implantation (PGA-macrofiber, PCL-nanofiber, and PDLGA-nanofiber) (Fig. 7).

DISCUSSION

SBS is a state of severe malabsorption and malnutrition, most often due to the surgical resection of the small bowel due to conditions such as volvulus, necrotizing enterocolitis, inflammatory bowel disease, cancer, or gastroschisis.[1] Nutritional support is often required due to malabsorption, the most severe consequence of SBS.[13] TPN has significantly improved survival but has severe complications. Catheter-related complications (including sepsis and thrombosis) and renal and liver insufficiency are associated with long-term TPN usage.[1,4,13] Approximately 15% of patients on long-term TPN ultimately progress to end-stage liver disease requiring transplantation for survival.[13]

Although intestinal adaptation may improve intestinal function by improving absorption by enterocytes and prolonging intestinal transit time, it cannot completely compensate for the loss of intestine.[13] Current surgical techniques used to increase absorptive surface area include longitudinal intestinal lengthening and tailoring (LILT) and serial transverse enteroplasty (STEP) procedures.[14] These procedures are indicated when there is failure to achieve

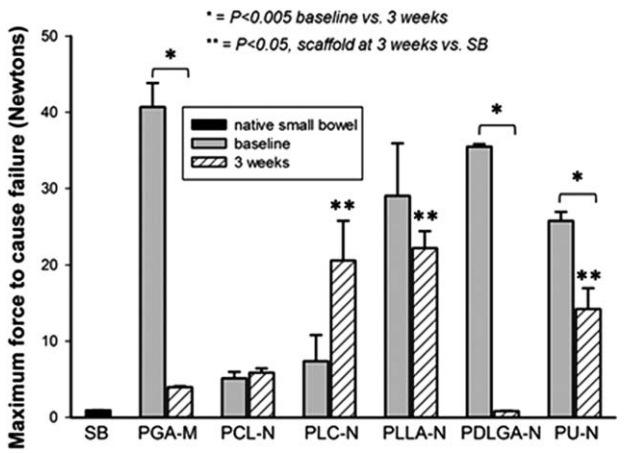

FIGURE 7. Suture retention strength. Suture strength measurements (in Newtons) for native small bowel and for scaffolds prior to and after 3 weeks of implantation. SB, small bowel; M, macrofiber; N, nanofiber.

intestinal autonomy by medical therapy alone, and may result in improved tolerance of enteral nutrition.[14] However, these procedures require significant dilation of the remaining intestinal segment, and often require repeat procedures. Transplantation is also of limited use due to the donor shortages, high costs, and the complications associated with long-term immunosuppression.[1,2,4,5] A more ideal tissue for intestinal replacement would be one that does not require immunosuppressive medications and can grow to become fully functional.[2]

Tissue engineering offers a promising alternative to current medical and surgical treatment of SBS. Tissue engineering involves seeding a scaffold made from a biodegradable polymer followed by either *in vivo* or *in vitro* incubation to allow for growth and differentiation of the cells to establish new, biocompatible tissue or organs.[1] The challenge has been to develop TEI that can be both functional and structurally similar to native small intestine.[15]

The peritoneal microenvironment plays an important role in the tissue engineering of small intestine. The peritoneal cavity has a microenvironment different than that of a subcutaneous location. The peritoneal membrane is highly vascularized, and this effect is augmented by conditions often triggering inflammation.[16] The pH of the peritoneal fluid ranges from approximately 7.5 to 8.0, and approximate ionic concentrations include: Na^{+} 145 mm/L, K^{++} 4.5–5.0 mm/L, Ca^{++} 0.8–1 mm/L, and HCO_3^{-} 30 mm/L.[16]

The polymers examined will ultimately be placed in continuity with the small intestine, and thus exposed to the luminal microenvironment of the small intestine. Once the scaffolds are anastomosed to the small intestine, they will be exposed to a number of additional factors that could affect their mechanical properties and rates of degradation. First, the pH in the small intestine increases from 6 to 7.4, as moving more distally.[17] Additionally, the scaffold will be exposed to a number of digestive enzymes, which are further activated by the basic environment of the small intestine.

Although the scaffolds in this study were not placed in direct continuity with the intestine, we did simulate the external peritoneal environment by placing the scaffolds in the peritoneal cavity as opposed to subcutaneous sites often previously reported. The expected harsher microenvironment of the small intestine led us to evaluate polymers having a wide variety of known properties to better anticipate the effects that both microenvironments may have on future TEI.

Scaffolds must be able to support the nutritional needs of arriving cells as they grow and proliferate.[4,15] In addition, biocompatibility requires that the scaffold produces minimal local or systemic host response.[7] Both synthetic and biologic materials, including acellular collagen-based matrices, have been used as templates for tissue engineering with mixed success.[18] Although biologic materials may have improved biocompatibility, we chose to analyze synthetic polymers due to the ability to optimize mechanical features of the scaffolds via a materials selection process.

Electrospinning of nanofibers for tissue engineering has a number of benefits.[19] These include cost-effectiveness[6,12] and that the scaffolds can be created in a nanoscaled form resembling the extracellular matrix allowing for more natural cellular proliferation.[3,6,15] Electrospinning also allows for the adjustment of fiber diameter and alignment to guide cellular infiltration. Pore sizes can also be adjusted and the scaffolds tend to have large surface areas with open, connected porous arrangements of 70%–90% relative porosity.[12] This allows for both enhanced drug delivery and room for cell adhesion and proliferation. Finally, multiple different polymers and blends of polymers can be used to create the ideal mechanical and degradative features for tissue engineering.[3] These alterations in scaffold structure allow for improved cell–scaffold interactions and may promote cell migration and proliferation to optimize the tissue engineered structure or organ. For these reasons, we chose to analyze electrospun nanofiber scaffolds made from six different polymers, and compare them to the commonly used PGA-macrofiber scaffold.

Degradation of synthetic polymers has been widely demonstrated as being faster *in vivo* compared with *in vitro*.[7] This is most likely due to the foreign body reaction to the scaffold resulting from the creation of a large "wound" and the presence of a foreign material in the abdominal cavity.[7] In addition, the factors of increased pH and different ionic concentrations of the peritoneal cavity would increase degradation. For example, PLGA-based scaffolds have been shown to produce acidic products during degradation that decrease the pH in the body's surrounding tissues, increasing the foreign body reaction.[6] These findings also demonstrate markedly increased degradation for the *in vivo* versus the *in vitro* environment.

Additionally, the higher surface-to-volume nature of nanofiber scaffolds has been shown to decrease foreign body reaction compared with non-nanofiber scaffolds.[6] In our histologic examination of scaffolds implanted in the abdominal cavity of the animals, the larger fiber diameter scaffolds (PGA-macrofiber and PCL-nanofiber) were associated with increased foreign body reaction. Similar to our PDLGA-nanofiber scaffolds, PLGA-based scaffolds cause minimal inflammation in previous literature.[20]

Ideally, the degradation rate of scaffolds should be slow enough to support the proliferation and differentiation of implanted cells while promoting the production of new ECM without restricting the eventual formation of new tissue. We show that the PGA-nanofiber scaffold degraded quite rapidly and thus was unable to be used for many of the evaluations, including SEM evaluation of fiber size, determination of tensile strength, or SRS. The PDLGA-nanofiber and PGA-macrofiber scaffolds exhibited more desirable degradation times that were slower than PGA-nanofiber but not nearly as long as the other scaffolds. It has been well documented that degradation of bulk PCL is slow, ranging from 2 to 4 years.[7] Similarly, PCL-nanofiber scaffolds showed little degradation during the *in vivo* implantation period. At 12 weeks PLC-nanofiber scaffolds displayed little degradation but did show a pronounced reduction in structural integrity.

Ultimate tensile strength is the highest point on the stress–strain curve, and represents the maximum amount of

stress that a material can withstand before failing. Young's modulus is the linear portion of the stress–strain curve, and corresponds to the ability of the scaffold to withstand alterations in length when exposed to tension. These factors are critical to the evaluation of scaffolds as they determine how the scaffold would respond to a bolus of food compared with the surrounding native small bowel. We have shown in previous study that deposited ECM and tissue infiltration has significant effects on the tensile properties of these nanofiber scaffolds.[21,22] The mechanical response of the scaffolds depends upon the alignment of the nanofibers in the direction of strain and the biological *milieu* can prohibit that fiber rearrangement.

In terms of tensile strength and suture retention testing, all scaffolds initially displayed equal or better strength and SRS than the native small bowel. PLLA-nanofiber and PDLGA-nanofiber were much stiffer than the other scaffolds. We hypothesize that the percent elongation was not statistically different as compared with the small bowel due to the relatively low strength of the small bowel compared with the PLLA-nanofiber and PDLGA-nanofiber scaffolds. This lack of stiffness has some benefit; however, in that it can help to maintain structural architecture during the formation of new tissues.[15] After 3 weeks of implantation, PGA-macrofiber and PDLGA-nanofiber most closely resembled the mechanical characteristics of small intestine, with PCL-nanofiber being the next closest in regards to mechanical characteristics of the small intestine.

In this specific environment, the PDLGA-nanofiber and PLLA-nanofiber scaffolds appear to strike the appropriate balance of properties needed to maintain structural integrity while allowing for the appropriate rate of tissue replacement of the synthetic scaffold. However, PDLGA-nanofiber appeared to be more biocompatible displaying a minimal foreign body response and a more ideal degradation rate. PU-nanofiber and PLC-nanofiber are much less ideal in this context due to their longer degradation rates, decreased porosity, and ongoing foreign body response. PCL-nanofiber caused significant tissue reaction but slower degradation making it appear less ideal. PGA-nanofiber scaffolds degraded too rapidly and did not allow sufficient ECM production, making it difficult to completely assess the state of the scaffold, as we were unable to test the characteristics of this scaffold. Finally, PGA-macrofiber causes significant tissue reaction but does have a more ideal degradation rate and tensile strength compatible with the production of TEI.

In summary, the results of this study indicate that scaffolds composed of PGA or PDLGA polymers may be preferable for the production of TEI. Electrospinning of nanofiber scaffolds may be the ideal format for constructing blended or layered polymers in order to produce a more biomimetic scaffold than is possible using a single material alone. Future studies to reassess these scaffolds after cell seeding, and after implantation in continuity with the small intestine, will provide additional information as to the relative ability of these polymers to support cells and allow efficient intestinal function while slowly being replaced by native tissue.

REFERENCES

1. Levin DE, Grikscheit TC. Tissue-engineering of the gastrointestinal tract. Curr Opin Pediatr 2012;24:365–370.
2. Levin DE, Dreyfuss JM, Grikscheit TC. Tissue-engineered small intestine. Expert Rev Med Devices 2011;8:673–675.
3. Rim NG, Shin CS, Shin H. Current approaches to electrospun nanofibers for tissue engineering. Biomed Mater 2013;8:014102.
4. Lalan S, Pomerantseva I, Vacanti JP. Tissue engineering and its potential impact on surgery. World J Surg 2001;25:1458–1466.
5. Langer R, Vacanti JP. Tissue engineering. Science, 1993;260:920–926.
6. Ji W, Yang F, Seyednejad H, Chen Z, Hennink WE, Anderson JM, van den Beucken JJJP, Jansen JA. Biocompatibility and degradation characteristics of PLGA-based electrospun nanofibrous scaffolds with nanoapatite incorporation. Biomaterials 2012;33:6604–6614.
7. Seyednejad H, Gawlitta D, Kuiper RV, de Bruin A, van Nostrum CF, Vermonden T, Dhert WJA, Hennink WE. In vivo biocompatibility and biodegradation of 3D-printed porous scaffolds based on a hydroxyl-functionalized poly(epsilon-caprolactone). Biomaterials 2012;33:4309–4318.
8. Sala FG, Matthews JA, Speer AL, Torashima U, Barthel ER, Grikscheit TC. A multicellular approach forms a significant amount of tissue-engineered small intestine in the mouse. Tissue Eng Part A 2011;17:1841–1850.
9. Gaumer J, Prasad A, Lee D, Lannutti J. Source-to-ground distance and the mechanical properties of electrospun fiber. Acta Biomater 2009;5:1552–1561.
10. Nam J, Huang Y, Agarwal S, Lannutti J. Materials selection and residual solvent retention in biodegradable electrospun fibers. J Appl Polym Sci 2008;10:1547–1554.
11. Chen JP, Su CH. Surface modification of electrospun PLLA nanofibers by plasma treatment and cationized gelatin immobilization for cartilage tissue engineering. Acta Biomater 2011;7:234–243.
12. Drilling S, Gaumer J, Lannutti J. Fabrication of burst pressure competent vascular grafts via electrospinning: Effects of microstructure. J Biomed Mater Res A 2009;88:923–934.
13. Seetharam P, Rodrigues G. Short bowel syndrome: A review of management options. Saudi J Gastroenterol 2011;17:229–235.
14. Frongia G, Kessler M, Weih S, Nickkholgh A, Mehrabi A, Holland-Cunz S. Comparison of LILT and STEP procedures in children with short bowel syndrome—A systematic review of the literature. J Pediatr Surg 2013;48:1794–1805.
15. Lee SJ, Atala A. Scaffold technologies for controlling cell behavior in tissue engineering. Biomed Mater 2013;8:010201.
16. Noh SM. Measurement of peritoneal fluid pH in patients with non-serosal invasive gastric cancer. Yonsei Med J 2003;44:45–48.
17. Fallingborg J. Intraluminal pH of the human gastrointestinal tract. Dan Med Bull 1999;46:183–196.
18. Qin HH, Dunn JC. Small intestinal submucosa seeded with intestinal smooth muscle cells in a rodent jejunal interposition model. J Surg Res 2011;171:e21–e26.
19. Lannutti J, Reneker D, Ma T, Tomako D, Farson D. Electrospinning for tissue engineering scaffolds. Mater Sci Eng C 2007;27:504–509.
20. Basu J, Mihalko KL, Payne R, Rivera E, Knight T, Genheimer CW, Guthrie KI, Sangha N, Jayo MJ, Jain D, Bertram TA, Ludlow JW. Regeneration of rodent small intestine tissue following implantation of scaffolds seeded with a novel source of smooth muscle cells. Regen Med 2011;6:721–731.
21. Johnson J, Ghosh A, Lannutti J. Microstructure-property relationships in a tissue engineering scaffold. J Appl Polym Sci 2007;104:2919–2927.
22. Johnson J, Niehaus A, Nichols S, Lee D, Koepsel J, Anderson D, Lannutti J. Electrospun PCL in vitro: A microstructural basis for mechanical property changes. J Biomater Sci-Polym Ed 2009;20:467–481.